Supporting Information: An Optofluidic System with Integrated Microlens Arrays for Parallel Imaging Flow Cytometry

Gregor Holzner, Ying Du, Xiaobao Cao, Jaebum Choo, Andrew deMello,*
and Stavros Stavrakis *

*E-mail: stavros.stavrakis@chem.ethz.ch, andrew.demello@chem.ethz.ch; Phone: +41 44 633 66 10

Department of Chemistry and Applied Biosciences, ETH Zürich, Vladimir Prelog Weg 1, 8093 Zürich, Switzerland
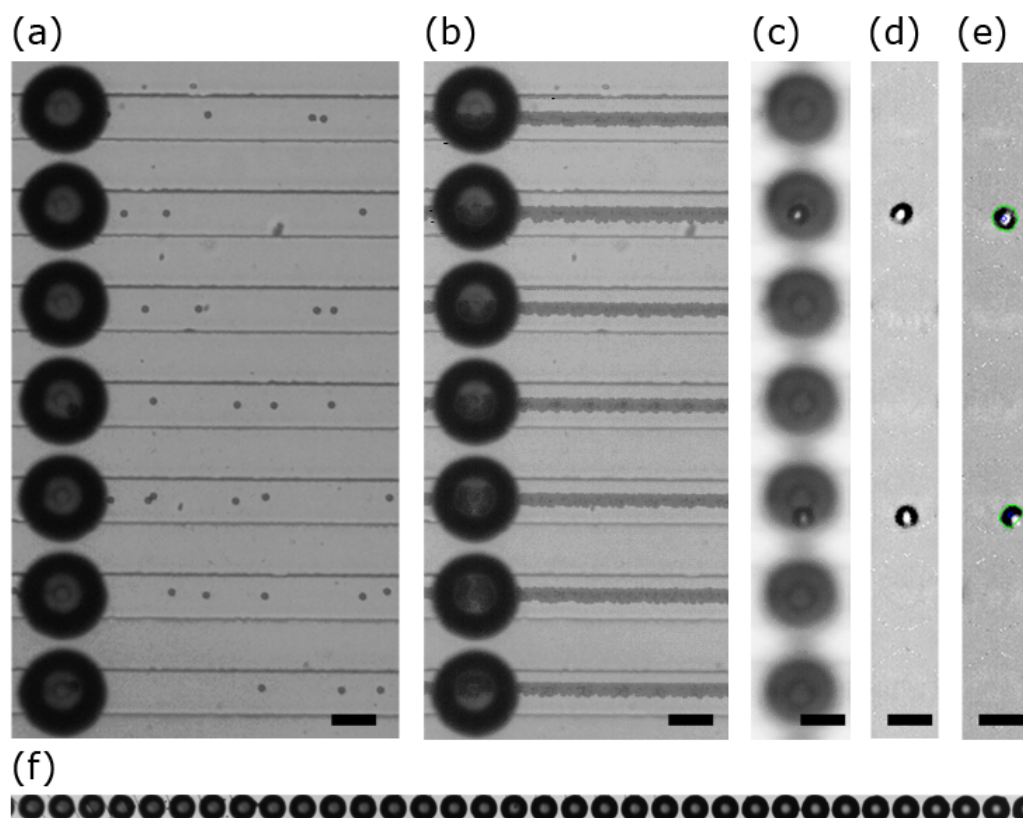
Figure S-1: (a) Image obtained with the objective lens focused on the 10 µm PS beads flowing through the microfluidic channel. (b) Image stack containing 1400 single images showing 10 µm PS beads flowing underneath the lenses. (c) Image showing beads flowing underneath microlenses at 3.5x magnification and (d) the same image after background subtraction. (e) After application of an image processing algorithm, detected beads are marked with a green contour. (f) An array of 34 microlenses within the field of view of a 4X objective. The scale bar represents 50 µm.

Supplemental Note S-1

Explanation of image processing steps

- **Background subtraction:** 1000 images are averaged (in ImageJ: Image/Stack/Z Project: Average Intensity). This average image is than subtracted from each individual image (in ImageJ: Process/Image Calculator: Operation: Subtract (32 bit result)). Followed by adjustment of contrast (ImageJ: Image/Adjust/Brightness/Contrast and conversion to 8bit (ImageJ: Image/Type/8bit).

- **Thresholding:** A binary threshold is applied to the background subtracted image (Python/OpenCV: cv2.threshold() yielding a binary image.) The threshold has to be adjusted manually to find either cells or beads. Within one set of experiments (e.g. cell experiment) the threshold is not changed.

- **Contour finding:** Contours are identified within the binary image (Python/OpenCV: cv2.findContours()).

- **Smoothing of contour:** by applying a convex hull transformation (Python/OpenCV: cv2.convexHull())

- **Contour clean up:** Removal of contours from aggregates, half imaged specimen, and debris by filtering contours due to their area (Python: if a1 < contour < a2: keep) and their roundness (area to circumference ratio).

- **Saving of parameters:** Frame number, position, area, perimeter of contour; intensity inside the contour. Save image with drawn contour for visual inspection.

(a)
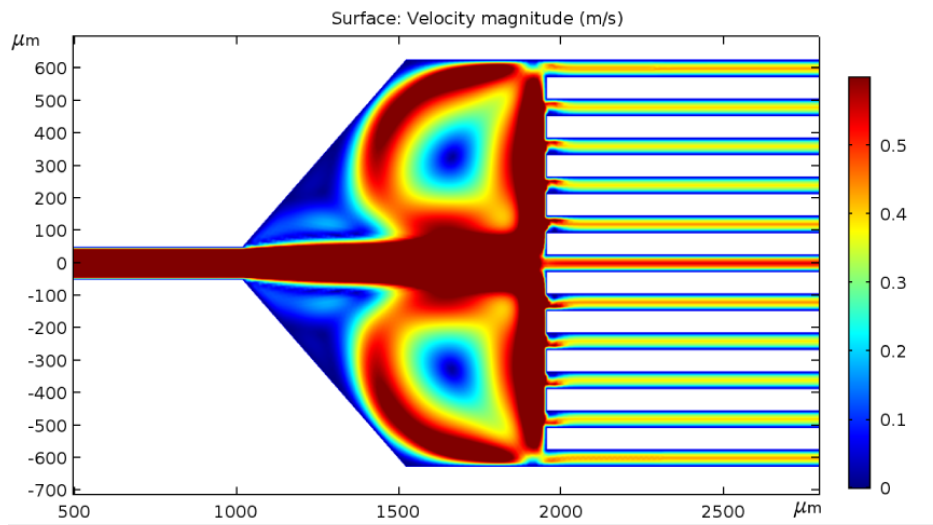
(b)
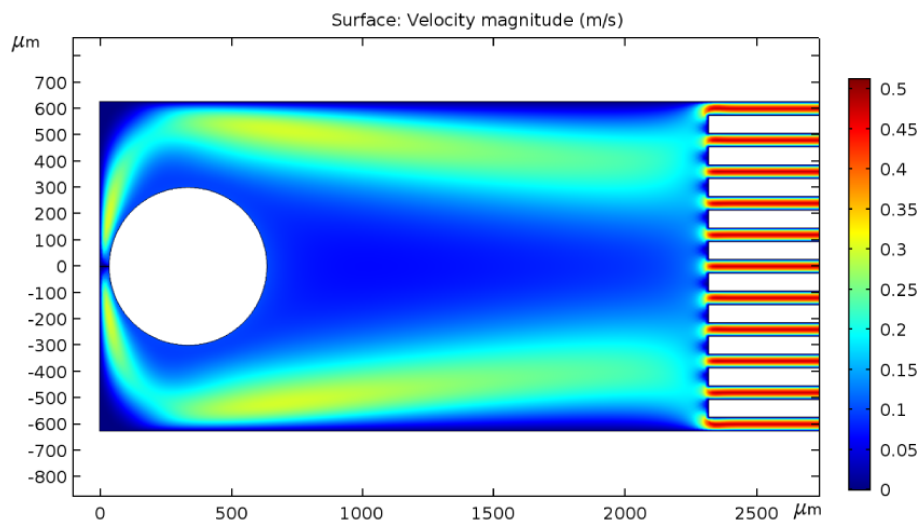
Figure S-2: COMSOL simulations depicting the flow distribution for two different chip geometries. (a) In the case where sample enters the microfluidic chip through a small channel, the flow distribution across the parallel channels is uneven. This phenomenon can be avoided as shown in (b) by directly punching the inlet hole (white circle) into a wider channel entrance.
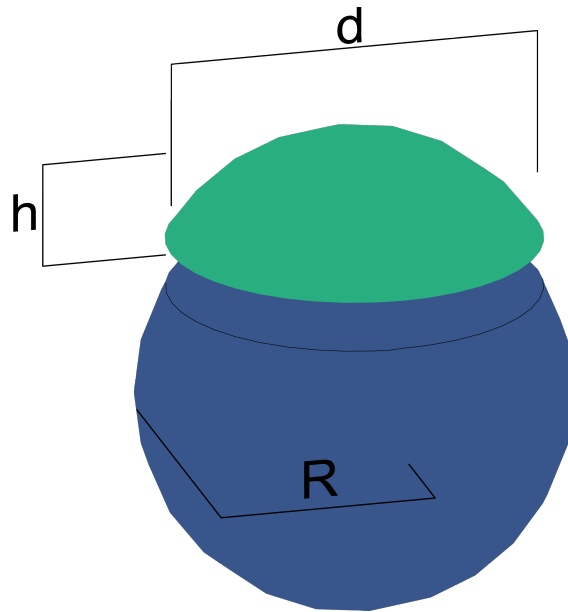
Figure S-3: Sketch highlighting the definitions of R, d and h as used in this work. R is the radius of the sphere (blue), also referred as the radius of the curvature; d is the diameter of spherical cap (green); h is the height of the spherical cap.

Da 1 = 112.6 µm
Db 1 = 9955. µm²
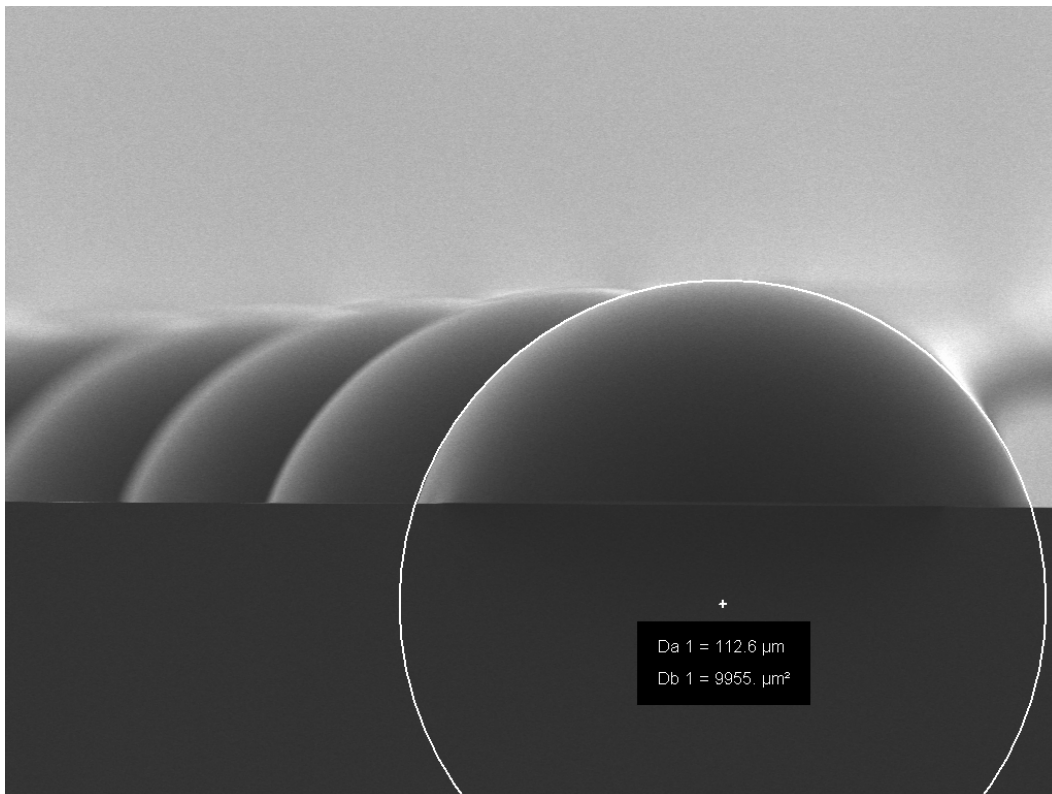
Figure S-4: SEM micrograph confirming that microlenses can be treated as spherical caps.
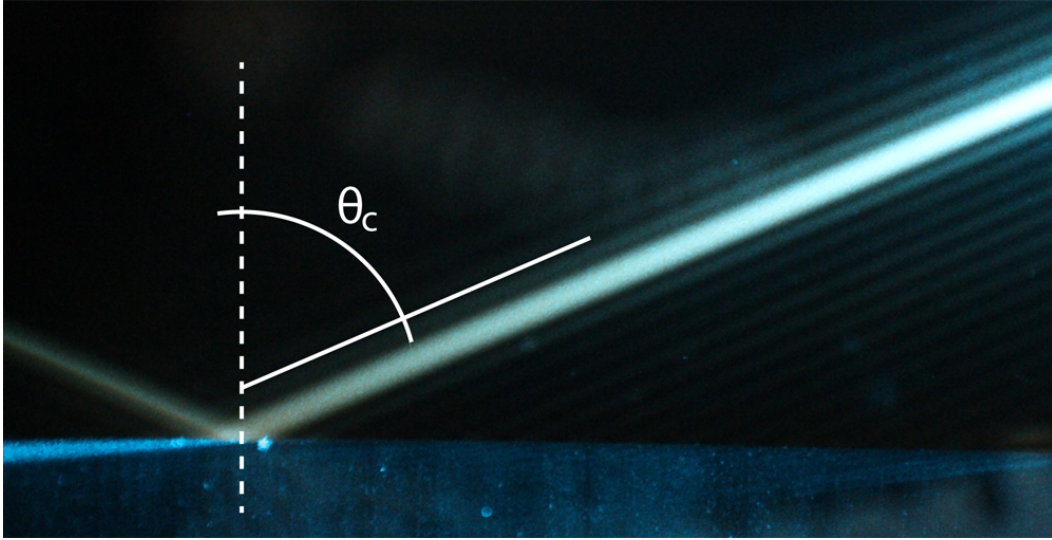
Figure S-5: Image of a 488 nm laser beam undergoing total internal reflection at the interface between cured AZ 40XT photoresist (the microlens material) and PDMS (n = 1.40[1]), whilst determining the critical angle, θ_c. Multiple measurements yield a value for θ_c of 23.47°. Since $\theta_c = arcsin(n_2/n_1)$, a refractive index of n $\approx$ 1.50 for the AZ 40XT photoresist is calculated. This measurement was performed using a flat piece of AZ 40XT with dimensions of 2×6×4 mm. It is noted that the measured refractive index is an approximation to the actual refractive index of a microlens due to the fact that during fabrication process microlenses experience different heating and cooling rates.
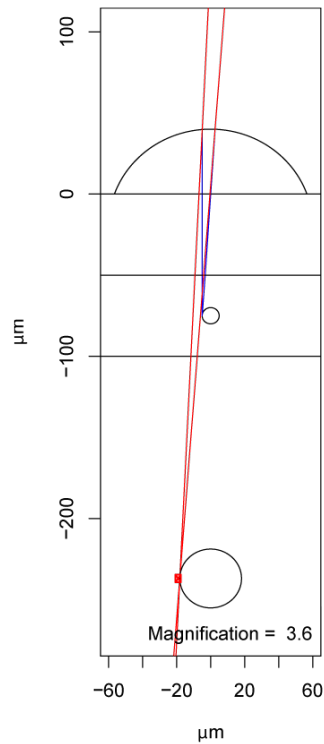
Figure S-6: (a) Ray tracing simulations predict a magnification of $\sim 3.6\times$, using experimentally determined dimensions and refractive index of the lens. A field of view of ~ 18 µm can efficiently image mammalian cells having an average size of 13 µm.

Table S-1: Refractive indices of materials used for simulations and calculations.

Material	n
Positive photoresist AZ 40XT	~ 1.52
36 % Optiprep solution[2]	1.314
PDMS[1]	1.400
Schott glass D263	1.523
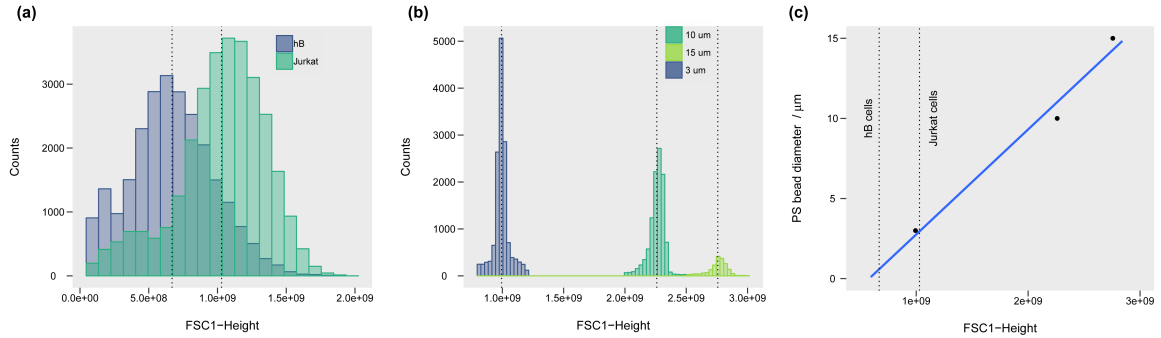
Figure S-7: (a) Forward scatter (FSC) signals (at 488 nm) of hB and Jurkat cells recorded using a commercial flow cytometer (Astrios MoFlo EQ, Beckman Coulter). Dashed lines indicate the mean FSC signal for each population. (b) FSC signals originating from three populations of polystyrene calibration beads; with average diameters of 3, 10 and 15 µm. (c) Variation of the FSC signal as a function of bead size diameter. Dashed lines indicate the mean signals for cell populations. Since, polystyrene beads will scatter differently to mammalian cells, signals originating from conventional FACS measurements primarily relate to the scattering properties of the cells rather than to their absolute diameters. Nonetheless, the gradient of the regression line indicates that hB and Jurkat cell diameters differ by 2.4 µm, a value that is in excellent agreement with our imaging flow cytometry measurements

References

(1) Whitesides, G. M.; Tang, S. K. Department of Chemistry and Chemical Biology, Harvard University 12 Oxford St., Cambridge, MA 02138. Proc. of SPIE Vol. pp 63290A–1.

(2) Axis-shield, OptiPrep™ Application Sheet. 2016; http://www.axis-shield-density-gradient-media.com/M01.pdf.